LANGMUIR

pubs.acs.org/Langmuir Article

Deposition of Nanometric Polymer−Surfactant Complexes Formed by Cationic Dextran: A Path to Sustainable Formulations

Hammad A. Faizi,*,# Daniel S. Miller,*,# Lyndsay Leal, Junsi Gu, Michaeleen L. Pacholski, Emmett M. Partain III, Caroline Nimako-Boateng, Janet R. McMillan, Chang Qian, Zuochen Wang, and Qian Chen

Cite This: *Langmuir* 2024, 40, 24360−24372 Read Online

ACCESS | Metrics & More | Article Recommendations | Supporting Information

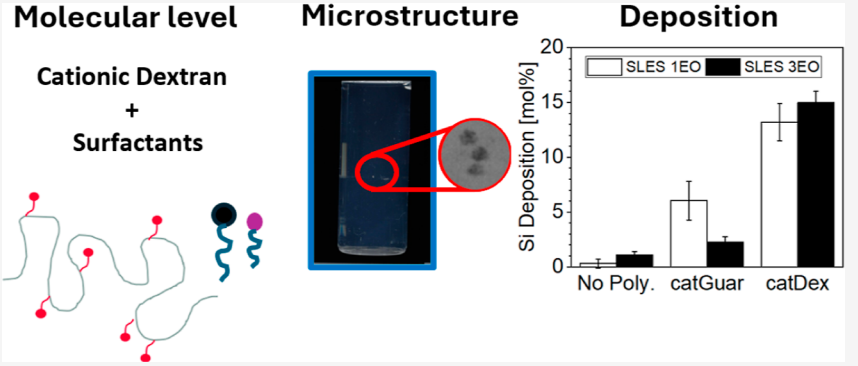

ABSTRACT: The home and personal care industry is evolving toward more sustainable and environmentally friendly ingredients. Rinse-off personal care products rely on formation of polymer−surfactant complexes to drive deposition of benefit agents (e.g., conditioning oils, fragrances, etc.) onto the skin or hair. The most used natural polymers for this purpose are cationic guar (catGuar) and cationic hydroxyethyl cellulose (catHEC), and the complexation of these polymers with surfactants has been rigorously characterized. Various gaps still exist with these polymers, specifically low biodegradation and undesirable aquatic toxicity profiles. Modified dextran offers an exciting solution as a biodegradable polysaccharide with a high natural origin content. This paper aims to compare the morphology of polymer−surfactant complexes formed between a cationic dextran (catDex) polymer with mixtures of sodium lauryl ether sulfate (SLES) and cocamidopropyl betaine (CapB) to the morphologies of complexes formed between catGuar or catHEC and the same surfactants. Solutions were designed to mimic industrially relevant shampoos. Through a suite of complementary techniques, unique nanometric sized complexes were observed to form between catDex−SLES/CapB compared to the widely reported micrometer-sized coacervates (liquid−liquid phase separation) or precipitates (liquid−solid) formed in catHEC or catGuar−SLES systems. Using a quartz crystal microbalance with dissipation, the adsorption behavior of the catDex−SLES/CapB is characterized on a silica-coated sensor. The results show deposition throughout the dilution regime for catDex−SLES/CapB where the highest deposition is recorded with the undiluted rinsing formulation. This contrasts with catHEC−SLES/CapB and catGuar−SLES/CapB where the highest deposition is recorded in phase-separated regimes. This result was extended to performance testing on hair, confirming that the unique complexes formed by catDex can drive remarkably high levels of silicone deposition from rinse-off personal care products. This innovative approach of utilizing catDex−SLES/CapB complexes could enable design of more sustainable formulations that rely on polycation−surfactant nanocarriers.

INTRODUCTION

Most ingredients in consumer goods are synthetically derived from petrochemicals, raising the concerns of fossil fuel depletion, greenhouse gas emissions, and water scarcity. For the past two decades, there is a drive for more eco-friendly ingredients which are biodegradable and bio sourced with low aquatic toxicity.[1,2] In this context, biopolymers, such as polysaccharides, are promising substitutes for synthetic ingredients, as they are widely available and diverse in chemical structure to allow flexibility in developing functional materials. While native polysaccharides can offer some benefits, many applications require the inclusion of cationic functionality to enhance the properties of the polymers. Commonly

Received: July 24, 2024
Revised: October 4, 2024
Accepted: October 28, 2024
Published: November 5, 2024

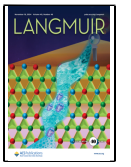

https://doi.org/10.1021/acs.langmuir.4c02860
Langmuir 2024, 40, 24360−24372

adopted functionalized natural polymers in personal care applications are cationic guar (catGuar) and cationic hydroxyethyl cellulose (catHEC), both quaternary amino-modified biopolymers. However, from a sustainability standpoint, various gaps still exist, specifically, the low biodegradation and undesirable aquatic toxicity profiles.

Cationic polysaccharides, including starches, guars, and cellulose derivatives, have been long studied as flocculants across a range of industrial sectors.[3,4] Of particular interest in this study is their use as polymeric additives in surfactant-rich systems to drive deposition or deliver hydrophobic materials to a substrate.[5−9] The phenomenon is widely leveraged in consumer formulations that contain hydrophobic oils or fragrances, such as laundry detergents and cosmetic products. Cationic hydroxyethyl cellulose and cationic guar gum are commonly used in the industry and have been well studied to form coacervates/precipitates with a variety of surfactants.[10−12] As described above, dextran offers an alternative backbone with high degradability and structural similarity to cellulose, both glucan-based polysaccharides.

Comparing the polysaccharide feedstocks of interest, cellulose and guar are harvested, while dextran is fermented from sucrose.[13] Cellulose is a highly rigid, linear polyglucan composed of glucose monosaccharides linked through (β-1,4) glycosidic bonds. Most commercial sources of cellulose are isolated from wood pulp or cotton linters and require functionalization for use in aqueous-based products. Guar gum, harvested from guar beans, contains two distinct sugar monomers, galactose and mannose, where mannose forms the backbone via (β-1,4) linkages, and alternating mannose repeat units are substituted with a pendent (α-1,6) galactose moiety. Like cellulose, dextran is a homopolymer of glucose, but the monosaccharides are connected through (α-1,6) glycosidic bonds, leading to high flexibility, low persistence length, and ready solubility in water.[14,15]

In general, polyelectrolyte−surfactant complexes form a variety of structures influenced by the properties of both components. Key factors include the chain stiffness, charge density, and molecular weight (MW) of the polyelectrolyte, as well as the packing parameter and headgroup type of the surfactant. These parameters determine the types of aggregates, such as micelles and vesicles, as well as size, shapes, and liquid crystalline phases of the polymer−surfactant complexes.[16,17] The structures evolve from individual surfactant molecules bound to polyelectrolytes to more complex formations like pearl-necklace structures, networks with rodlike micelles, multilamellar vesicles, and nanorod assemblies.[18−21]

While polyelectrolyte−surfactant complexes formed by catGuar and catHEC polymers have been extensively characterized previously,[4,6,7,22−24] only limited studies have been published on complexes formed between cationically modified dextran (catDex) polymers and surfactants. Most of the prior work in the area was motivated by use of catDex polymers as flocculants for water treatment and mining and drug delivery vehicles.[25,26] Of key interest to the present work, both self-assembly of dextran functionalized with *N*-alkyl-*N*,*N*-dimethyl-*N*-(2-hydroxypropyl) ammonium chloride and the association of these cationic dextran polymers with surfactants have been rigorously characterized by microcalorimetry, conductivity, UV−vis spectrophotometry, viscometry, and fluorimetry.[27−32] Nichifor et al. systematically characterized the association of a 40,000 Da MW dextran polymer functionalized with *N*-alkyl-*N*,*N*-dimethyl-*N*-(2-hydroxypropyl) ammonium chloride, where the alkyl chain lengths were 2, 4, 8, 12, or 16 carbon atoms, with sodium alkyl sulfates, where the alkyl chain lengths were 8, 10, 12, 14, or 16.[31] The researchers compared complexation events to the critical association concentration of the polymer (CAC_P) and the critical association concentration of the surfactant (CAC_S). At polymer concentrations below CAC_P and surfactant concentrations above CAC_S, binding of the surfactant by the polymer is induced by the presence of hydrophobic functionalities on the polymer, which can become wrapped by surfactant micelles. At polymer concentrations above CAC_P and surfactant concentrations above CAC_S, interpolymer−surfactant complex associations can occur where complexes contain multiple polymer chains associated with multiple surfactant micelles.

At polymer concentrations below CAC_P and surfactant concentrations below CAC_S, surfactant unimers associate with the polymer chains, and the properties of the polymer−surfactant complexes are like those of polymer aggregates in the absence of surfactant. If enough surfactant is present, micelles can also nucleate around hydrophobe functionalities on the polymer. This is the widely reported apparent critical aggregation concentration in polymer/surfactant mixtures where micelles nucleate at concentrations below CAC_S.[33] At polymer concentrations above CAC_P and surfactant concentrations below CAC_S, the complexation is driven by interpolymer association. Whether surfactant unimers or micelles are present in complexes will depend on the concentration of surfactant in the system.

Overall, these past studies highlight the rich variety of polymer−surfactant complexes that can form in systems that contain both cationically modified dextran polymers and anionic surfactants. The present research expands these studies in two ways. First, we investigate the morphology and deposition of a high MW cationically modified dextran, which is hypothesized to have increased levels of polymer−surfactant complexation and, thus, improved delivery of benefit agents from rinse-off personal care formulations to the skin or hair. Second, we focus our efforts on surfactant mixtures containing anionic and neutral surfactants used in many industrially relevant applications, such as shampoos, conditioners, and detergents. Specifically, we investigate the complexation of the cationically modified dextran polymers with mixtures of sodium lauryl ether sulfate (SLES) and cocamidopropyl betaine (CapB).

Below, we compare the complexes formed between catDex polymers and mixtures of SLES and CapB to those formed between catGuar or catHEC and the same surfactant mixtures. We first present operating diagrams for each of the cationic polysaccharides mixed with relevant personal care surfactants to outline practical formulation conditions under which complexes are formed. To complement these operating diagrams, we next present the appearance of model shampoos throughout a relevant dilution process. We next provide insights into the size and morphology of catDex−surfactant complexes by dynamic light scattering (DLS) and liquid-phase transmission electron microscopy. We hypothesized that the catDex−surfactant complexes could both deposit effectively onto surfaces and drive the deposition of benefit agents to hair from rinse-off personal care formulations. Thus, we next present the adsorption behaviors of the complexes onto silica-coated sensors by a quartz crystal microbalance with

https://doi.org/10.1021/acs.langmuir.4c02860
Langmuir 2024, 40, 24360−24372

dissipation (QCM-D). Finally, we demonstrate that the catDex polymers can increase the deposition of silicone from a model shampoo compared with the catHEC and catGuar technologies. Overall, the results presented here will guide formulation of products that rely on polycation−surfactant complexes to benefit the skin/hair or deposit benefit agents onto them.

MATERIALS AND METHODS

Materials. Max 60 FlackTek cups were purchased from FlackTek Inc. (Greenville County, South Carolina, USA). 38 mm (2 ounce) clear plastic cups were purchased from Parkway Plastics Inc. (Piscataway, New Jersey, USA). FlackTek or Parkway cups were used interchangeably throughout the study. Wheaton one-ounce glass vials, eight-ounce glass jars, micropipettes, pipet tips, and transfer pipettes were obtained from Fisher Scientific (Waltham, Massachusetts, USA). STEOL CS-130 (SLES 1EO), STEOL CS-330 (SLES 3EO), AMPHOSOL CA (CapB), and BIOSOFT N-300 (TEA-DDBS) were obtained from Stepan Company (Northbrook, Illinois, USA). Jaguar Excel (catGuar; Lot MJAX17181A) was obtained from Solvay S. A. (Neder-Over-Heembeek, Brussels, Belgium). UCARE JR-30 M Polymer (catHEC) and DOWSIL 1785 POE Emulsion were obtained from Dow Inc. (Midland, Michigan, USA). Experimental catDex polymer prototypes were prepared internally by Dow (Collegeville, Pennsylvania, USA). A summary of notable parameters of the polymers used are described in Table 1.

Table 1. Overview of Cationic Polysaccharides Used in the Present Study[a]

property	catHEC	catGuar	catDex
molecular structure	β-1,4 glucose	β-1,4 mannose with alternating 1,6 galactose	α-1,6 glucose
approximate MW [MDa]	1.0	1.0	0.2−0.5
approximate charge density [meq/g]	1.3	0.7	1.1
approximate persistence length of backbone [nm]	29	10	0.7

[a]Persistence length values taken from the previous literature.[14,15]

Model Shampoo Formulation. The model formulation developed as part of this study is shown in Table 2. The primary and secondary surfactants used in the shampoos are SLES and CapB, respectively. SLES is an efficient cleaning surfactant and the inclusion of EO units between the sulfate and lauryl group both improves oil solubilization and imparts mildness relative to sodium lauryl sulfate (SLS).[34] Inclusion of CapB increases the mildness of shampoos to the eye and skin and helps to build viscosity in combination with added salt.[35,36] It is common to include emulsified benefit agents into shampoos for conditioning purposes.[7,9] One such beneficial agent is silicone. In this study, we excluded silicone emulsions. However, TEA-DDBS (triethanolamine dodecylbenzenesulfonate) was included in the model formulations to simulate the anionic surfactant stabilizer that would enter the shampoo with the silicone emulsion. This is following the convention of related studies.[7,9]

Table 2. Model Shampoo Formulation Used in the Present Study to Enable Fundamental Research

name	description	wt % in product	wt % in formulation
water		100	balance
STEOL CS-130 or STEOL CS-330	primary surfactant: cleaning	30	9.00%
cationic polymer	deposition aid	100	0.30%
AMPHOSOL CA	co-surfactant: foam booster and viscosity builder	35	2.00%
neolone PE preservative	preservative	50	0.25%
BIOSOFT N-300	silicone emulsion stabilizer	60	0.12%

The shampoos were prepared by first adding polymer to Max 60 Long FlackTek cups. Then, surfactant solutions and water were added. Finally, the shampoo was mixed for 2 min at 1950 rpm using a SpeedMixer (FlackTek, Inc., Landrum, South Carolina, USA) and placed on a hematology mixer (Medmark Technologies LLC, Perkasie, Pennsylvania, USA) to further mix overnight. All shampoos were visually inspected to ensure complete hydration of the polymer prior to dilution with water.

Operating Diagram Measurements. Many of past studies have measured phase diagrams for mixtures of cationic polymers and anionic surfactants.[24,37−40] Here, we chose to limit the regions explored in the compositional space to those relevant for commercial rinse-off personal care products. For this reason, we refer to our measurements as "operating diagrams" rather than as phase diagrams.

Two types of operating diagram studies were conducted. Like the past phase behavior studies,[24,37−40] the first type involved formulating to a single point in polymer−surfactant compositional space. The samples for this type of study were prepared by first making separate stock solutions of polymers in water and surfactants in water. The stock solutions of polymer in water were prepared at 2 wt % prior to dilution. Polymers were allowed to hydrate by mixing for 2 min at 1950 rpm in a SpeedMixer (FlackTek, Inc., Landrum, South Carolina, USA) and subsequently rolling the stock solutions overnight on a hematology mixer (Medmark Technologies LLC, Perkasie, Pennsylvania, USA). Complete hydration of the polymer was confirmed by observing the uniform appearance of the sample prior to use. The stock solutions of surfactant in water contained SLES 1EO, CapB, and TEA-DDBS. They were prepared at fixed mole ratios of CapB to total surfactant and TEA-DDBS to total surfactant of 0.176 and 0.008, respectively. Again, uniform stock solutions were confirmed prior to use.

Once the stock solutions were prepared, five gram samples were made by dispensing the stock solutions and water into compression sealed screw cap vials using a Hamilton Microlab Star liquid handling robot (Hamilton Company, Reno, Nevada, USA). The order of addition was water, surfactant stock, and finally polymer stock. After preparation, the screw cap vials were capped and mixed using an Eberbach fixed-seed reciprocal shaker (Eberbach Corporation, Belleville, Michigan, USA). The samples were imaged after mixing and periodically over six months to track their appearance over time. The imaging was conducted using the Dow custom Phase Identification and Characterization Apparatus (PICA) robot, which moves vials from a temperature-controlled deck to an imaging chamber to capture photographs in a one-by-one fashion using a robotic arm.

The second type of operating diagram study sought to simulate dilution of a model shampoo in use and was an adaptation of a previously described workflow.[41] First, thirty gram quantities of model shampoos were prepared as described above. The model shampoos contained 9 wt % SLES 1EO or SLES 3EO, 2 wt % CapB, 0.12 wt % TEA-DDBS, and 0.3 wt % of cationic polysaccharide. Dilutions of these model shampoos were then performed on a volumetric basis. The dilutions used were 1-fold (i.e., 1 part shampoo, 1 part DI water), 2-fold, 5-fold, 10-fold, or 20-fold. Following dilution, photographs of the samples were taken by using the PICA robot. A so-called "PIC-SHAKE-PIC" method was used that involves taking a picture, shaking the vial for 15 s using an automated wrist shaker, and taking another picture immediately after mixing. Additional photographs were taken 24 h after mixing.

Measurement of Micelle Microstructure via DLS. Samples were prepared for DLS measurements by first adding water to 1 ounce vials on a balance. Then, SLES stock was added using a micropipette. Next, CapB and TEA-DDBS stocks were added. Following the surfactant additions, the vials were capped and vortex mixed for 10 s at 3000 rpm. Following mixing, the sample aliquots were transferred to DLS cuvettes. DLS measurements were performed using a Malvern ZetaSizer Nano ZS instrument (Malvern Panalytical, Malvern,

https://doi.org/10.1021/acs.langmuir.4c02860
Langmuir 2024, 40, 24360−24372

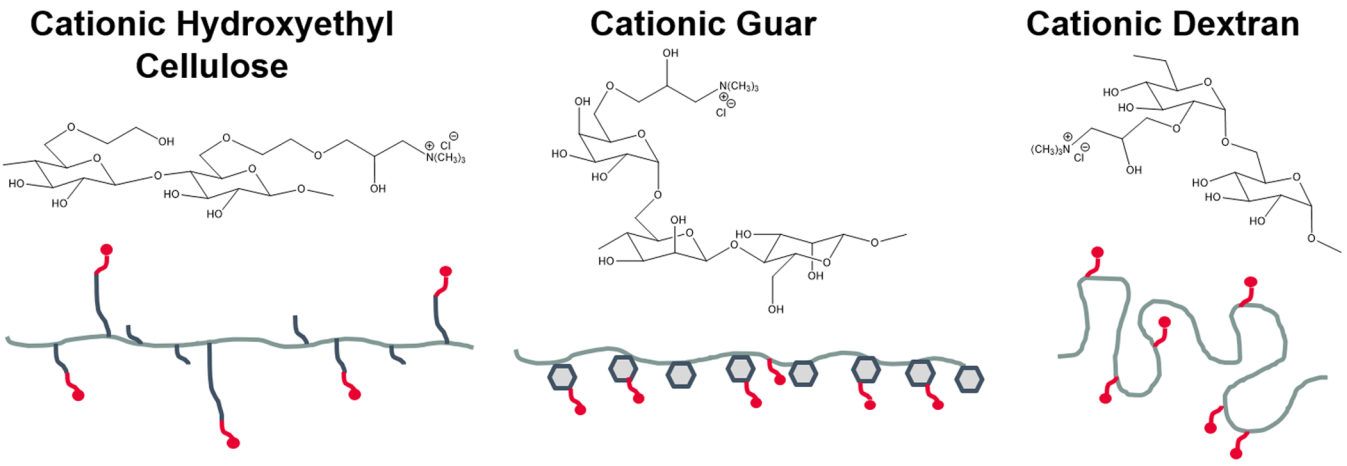

Figure 1. Idealized chemical structures of the repeat units of the cationic deposition aid polymers used in 2-in-1 shampoos studied. The polymers studied were catHEC, catGuar, and catDex.

Worcestershire, United Kingdom). To predict the colloidal stability of the complexes, ZetaSizer Nano ZS was used to determine the zeta potential (ζ) of catDex−SLES/CapB solution utilizing the Smoluchowski model at 25 °C.[42] The solution based on Table 2 was diluted 2-fold with DI water before measurement.

Liquid-Phase Transmission Electron Microscopy Image Acquisition and Image Analysis. The liquid-phase transmission electron microscopy (TEM) imaging was performed by using a Talos F200X G2 200 kV FEG scanning transmission electron microscope and an electrochemical liquid flow TEM holder (Protochips). The SiNx microchips used in our experiments were purchased from Protochips (Morrisville, North Carolina, USA), where the dimensions can be described as 150 nm spacer; bottom microchip window size: 50 μm × 550 μm × 50 nm (EPB-55DNF-10); top microchip window size: 50 μm × 550 μm × 50 nm (EPT-55W-10). The microchips were immersed in acetone and methanol for 3 min, respectively, in sequence to remove the protective polymer layer. The SiN_x side was treated with oxygen plasma (Harrick Plasma Cleaner PDC-23G) at low RF level for 27 s to clean the surface for enhanced hydrophilicity right before the chip assembly. The liquid-phase TEM image and movies were captured by a Ceta 16 M camera. The images were captured with an exposure time of 1 s, and the movies were captured with a frame rate of 5.7 fps and 0.15 s exposure time. The dose rate utilized was 7.94 e^{-} $Å^{-2}$ s^{-1}. The complexes were stable under the beam illumination, which did not show any shape change after 10 min movie capturing.

The image analysis was based on the homemade MATLAB code. We used the MATLAB function 'imbinarize.m' to binarize the images based on a locally calculated adaptive pixel intensity threshold, to differentiate the complexes from the background. Occasionally, multiple particles were aggregated and recognized as connected features by the algorithm, which were manually separated. The shape parameters such as the area, length of the major axis, and aspect ratios of the complexes were then obtained from the segmented images using the MATLAB function.

QCM-D Monitoring. QCM-D measurements were performed with a QSense Analyzer (Biolin Scientific) using SiO_2-coated sensors purchased from Biolin Scientific Instruments (QSensors QSX 303). The sensors were cleaned using the recommended manufacturers' sensor cleaning protocol to obtain stable and reproducible baselines. This step consisted of submerging the sensor in a 2 wt % aqueous sodium dodecyl sulfate (SDS) solution for 30 min. The sensor was rinsed by ultrapure water and dried by a stream of nitrogen gas. The sensor was treated for 15 min with UV/ozone (Biolin ESA006, UV/ozone cleaner). For a typical measurement, an Ismatec Digital Peristaltic pump equipped with 0.91 mm Tygon tubing was utilized for continuous flow of solution over the sensor 0.1 mL/min at 20 °C (PTFE tubing was used to connect the reservoir solution, QCM sensor module, and pump tubing). Initial baseline conditions were set with ultrapure water flow for 30 min. For experiments where shampoo was introduced, frequency data was collected continuously, and the pump flow paused briefly to exchange feed solutions from an ultrapure water flow.

The complex shear modulus of the film is defined by

$$G = G' + iG'' = \mu_f + 2\pi i f \eta_f = \mu_f(1 + 2\pi i f \tau_f)$$

where μ_f is the elastic shear or storage modulus, η_f is the shear viscosity or loss modulus, f is the oscillation frequency, and τ_f is the characteristic relaxation time of the film. The viscoelastic properties of the adsorbed film were determined by a model presented by Voinova et al.[43] where the film is represented by a single Voigt element. In this case, the quartz crystal is assumed to be a purely elastic material surrounded by a purely viscous and Newtonian solution. Furthermore, the thickness d_f and the density ρ_f of the film are uniform and the viscoelastic properties are assumed to be frequency independent with no slip between the adsorbed layer and crystal. Results from measurements at several overtones were fitted to this model by using the program D-find from QSense (Biolin Scientific).

Silicone Deposition Studies on Washed Hair Tresses. Caucasian virgin hair from International Hair Importers was used for testing the silicone-containing shampoos. Each tress weighed about 2 g. To clean and strip each tress, the tress was rinsed for 30 s under a stream of tap water, and then 0.4 g of a solution containing nine percent of sodium lauryl sulfate was applied and lathered through each tress for 30 s. The structures were then rinsed for 1 min under running water. Excess water was removed from the tresses by passing each tress between the index and middle fingers of the hand. The tresses were then treated with the model formulation from Table 1 with 1 wt % of DOWSIL 1785 POE Emulsion at 0.4 g formulation/g of hair by massaging the formulation into the wet/damp hair for 1 min. The layers were then rinsed for 30 s under running water and allowed to dry overnight at room temperature.

X-ray Photoelectron Spectroscopy. Samples were analyzed as received by taping sections of hair tresses to double-sided tape. Data were taken from regions in which no underlying tape was optically visible. X-ray photoelectron spectroscopy (XPS) gives quantitative elemental and chemical state information from the top 10 nm. XPS data were acquired from four areas across 1 cm × 3 mm from the center of the tress. Instrument parameters can be found below. XPS data are reported as the average and standard deviation of those data points. Data were acquired using a Thermo K-alpha XPS instrument with a monochromatic Al K-alpha X-ray source and 90° take off angle. Survey spectra were acquired at 200 eV pass energy: elements identified were analyzed with a 20 eV pass energy in scan mode for quantification using Thermo sensitivity factors. For all data collection, charge compensation was used as well as a 400 μm X-ray spot size.

https://doi.org/10.1021/acs.langmuir.4c02860
Langmuir 2024, 40, 24360−24372

Data were analyzed using Casa 2.3.17 Dev 6 3y with a linear background.

RESULTS AND DISCUSSION

Characterization of Polymer−Surfactant Complexes. The first step toward understanding the complexes that can form between catDex, catGuar, or catHEC polymers and surfactants used in rinse-off personal care products was to measure polymer−surfactant operating diagrams that track the optical appearances of samples as a function of the composition of polymer and surfactants.[34] The surfactants selected for the operating diagrams were SLES 1EO, CapB, and TEA-DDBS, which are commonly used in shampoo formulations. The mole ratios of CapB to total surfactant and TEA-DDBS to total surfactant were fixed at 0.176 and 0.008, respectively. We hypothesized that both differences in persistence lengths of the polymer backbones (Table 1) and the differences in the proximity of the cationic functionalities to the polymer backbones (Figure 1) would result in different polymer−surfactant complex morphologies. Consistent with this hypothesis, Figure 2 shows that three distinct operating diagrams were measured for the three polymers.

Figure 3 shows representative examples of the three types of sample appearances observed. The first appearance was a clear liquid. The second appearance was a blue turbid solution like that described by Miyake and collaborators.[44,45] The third and final appearance was a solid−liquid phase separation, where a solid precipitate was observed to deposit onto the bottom of the vials.

On each of the operating diagrams, an approximate charge neutralization line is provided based on the amount of SLES 1EO in the system (see ESI for details). The charge neutralization lines will be slightly below the lines provided because CapB can partially neutralize the charge of SLES. Of note, the region of interest to rinse-off personal care products is below the approximate charge neutralization line because, in these systems, the surfactant concentrations are higher than those of the polymers. Interestingly, the operating diagram for the catDex polymer shows that there was a wide formulation window over which the blue turbid solution was observed. As shown in Table 1, the MW of the catDex polymer was lower compared to those of the catGuar and catHEC polymers. The lower MW catDex polymer was chosen, because it is more industrially relevant. For the purposes of this study, we also verified that the blue turbid solutions could be obtained with a high MW catDex polymer (MW = 1.0−2.0 MDa) at the same charge density. The data present in the ESI (Figure S4) verifies that formation of the blue turbid solutions was not the result of lower MW qualitatively, as the solutions were also observed for the high MW catDex polymer.

We also studied the impact of the mode of preparation of samples on formation of the blue turbid solution because polymer−surfactant complexes can be influenced by preparation parameters such as rapid mixing, slow dropwise addition, or even order of addition.[46,47] As outlined in the ESI, the blue turbid phase solution was obtained independently of the order of addition or different mixing speeds. Electrophoretic mobility measurements of freshly prepared catDex−SLES 1EO/CapB and catDex−SLES 3EO/CapB displayed negative ζ-potential values of -23.3 ± 0.3 and -20.7 ± 2.0 mV, respectively. When combined with the long-term shelf life stability (e.g., at least stable for over six months as determined for this experiment) and the negative charge of complexes in freshly prepared solutions, we interpret these results to indicate that the blue turbid phase solution is likely caused by long-term stable or kinetically trapped complexes.

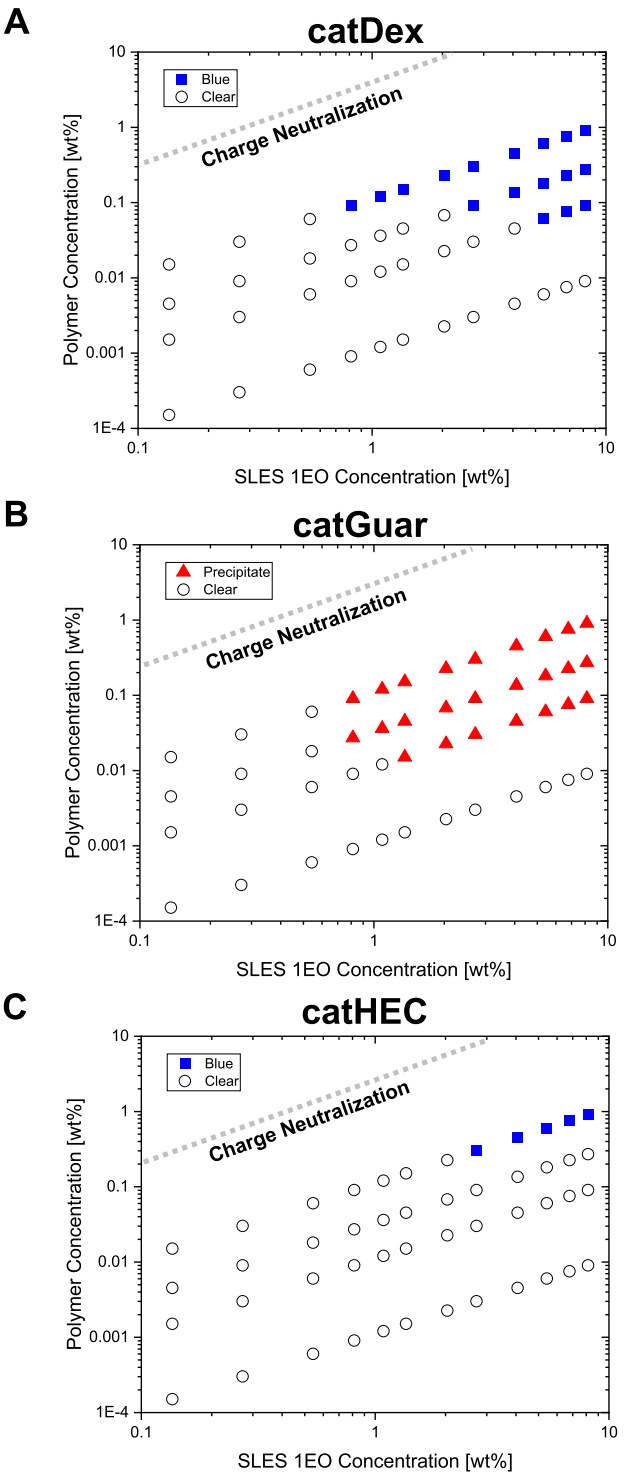

Figure 2. Polymer−surfactant operating diagrams for (A) catDex, (B) catGuar, and (C) catHEC. In addition to SLES 1EO, the samples also contained CapB and TEA-DDBS. The mole ratio of CapB to total surfactant was 0.176, and the mole ratio of TEA-DDBS to total surfactant was 0.008. The dashed lines indicate charge neutralization between the respective cationic polysaccharide and anionic surfactants. Black open circles indicate a clear liquid, blue squares indicate a blue turbid solution, and red triangles indicated a liquid−solid phase separation.

https://doi.org/10.1021/acs.langmuir.4c02860
Langmuir 2024, 40, 24360−24372

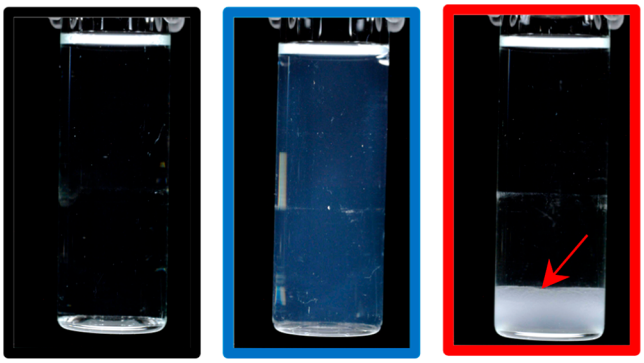

Figure 3. Classification of sample appearances observed during measurement of polymer−surfactant operating diagrams: (left) clear liquid; (middle) blue turbid solution; and (right) liquid−solid phase separation. The red arrow points to the solid precipitate observed at the bottom of the sample. The colors outlining the images correspond to the observations reported in Figure 2. The concentrations of anionic surfactant and cationic polymer in each of the samples were: (left) 100 mM SLES 1EO/0.1 wt % catHEC; (middle) 300 mM SLES 1EO/0.3 wt % catDex; and (right) 100 mM SLES 1EO/0.3 wt % catGuar. The contrast of the images was enhanced to highlight the blue hue. The original images are provided in Figure S1 of the ESI.

The behavior of the catGuar system was strikingly different from that of the catDex system. Only a solid−liquid phase separation was observed for the catGuar system over the compositional space studied.[48] This was observed with both SLES 1EO and SLES 3EO shampoos. Thus, if a blue turbid solution exists for this polymer, the stability window was so narrow that we did not observe it. Over the industrially relevant concentrations studied, and consistent with the observations of Miyake and Kakizawa,[44,45] a blue turbid solution was observed over a very narrow window in compositional space for the catHEC system. Thus, a key observation gleaned from Figure 2 is that the structure of the catDex polymer promotes a wide formulation window over which a blue turbid solution can be obtained relative to the other two polymers.

The operating diagrams shown in Figure 2 were measured by formulating to a single point in the compositional space. In practice, rinse-off personal care products are used by formulating to a single point in compositional space and diluting continuously with water. As pointed out by Wagner and collaborators, such a process can result in kinetically trapped states at relevant use conditions.[24] Thus, we next sought to characterize differences in sample appearances observed when this method is followed. Figure 4 shows dilution series for model shampoos formulated with 9 wt % SLES 1EO or SLES 3EO, 2 wt % CapB, 0.12 wt % TEA-DDBS, and 0.3 wt % of the indicated cationic polysaccharide. SLES 3EO was added to this experiment for comparison, because it is also commonly used in rinse-off personal care formulations. The dilutions were done on a volumetric basis and were one-fold (i.e., 1 part shampoo, 1 part DI water), 2-fold, 5-fold, 10-fold, or 20-fold.

For the model shampoos containing catDex, the blue turbid solution was observed in both SLES 1EO and the SLES 3EO system. It was slightly more pronounced in the SLES 1EO system. As the catDex-containing shampoos were diluted, the blue turbid appearance became less visible; with the samples appearing "water clear" at a 5-fold dilution. At this point, it was unclear if this was caused by dissociation of complexes or reduced light scattering due to dilution of the complexes. This was investigated further and is described below.

Figure 4 shows that the solid−liquid phase separation observed in the catGuar operating diagram shown in Figure 2 also appeared during the dilution of both SLES 1EO and SLES 3EO shampoos containing catGuar. Solid precipitate was observed to deposit onto the bottom of the sample vials between 2-fold and 10-fold dilutions consistent with the previous literature.[23,26,40−42] Such precipitation is thought to drive deposition of the polymers themselves and/or drive deposition of benefit agents included in the shampoos.[6,7,9,48] Interestingly, a faint blue turbid appearance was observed in the undiluted shampoos containing catGuar. The turbidity was lower than that observed for the shampoos with catDex. This indicates that, like the catHEC system, there is a narrow formulation window over which blue turbid solutions can be obtained with catGuar. The region where these solutions can be obtained is slightly to the right of the precipitate region studied in Figure 2.

A very faint blue turbid solution was also observed for the catHEC-containing SLES 1EO model shampoos. The blue turbid solution was much less turbid in the shampoos containing catHEC compared with those containing catDex. As was the case with the catDex-containing model shampoos, the blue turbid appearance was observed to disappear upon dilution. In contrast to the shampoos containing catGuar, no solid−liquid phase separation was observed in shampoos containing catHEC. We hypothesize this is because the galactose branch points on the rigid catGuar backbone lead

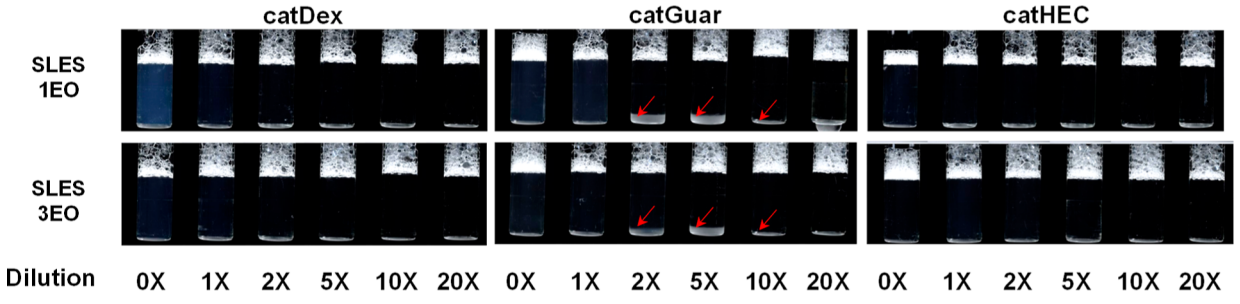

Figure 4. Photographs of model shampoos throughout dilution with deionized water. The undiluted shampoos (marked as 0 ×) contained 9 wt % SLES 1EO or SLES 3EO and 2 wt % CapB, 0.12 wt % TEA-DDBS, and 0.3 wt % cationic polysaccharide. The polymers are indicated above each panel: (left) catDex, (middle) catGuar, and (right) catHEC. The dilution is factor is given below each image on a volume basis. The red arrow points to the solid precipitate observed at the bottom samples containing catGuar. The contrast of the images was enhanced to highlight the blue hue. The original images are provided in Figure S2 of the ESI.

https://doi.org/10.1021/acs.langmuir.4c02860
Langmuir 2024, 40, 24360−24372

to strong interactions between hydroxyl groups and oxyethylene units with even low EO SLES leading to associative phase separation. The catHEC polymer has no such branch points, and direct interaction with the anhydroglucose backbone may be disrupted by the ethylene oxide functionalities.

Overall, there were distinct differences among the systems containing each of the three cationic polysaccharides. For model SLES 1EO shampoos, the catGuar systems showed a propensity for solid−liquid phase separation at concentrations relevant to formulation of rinse-off personal care products. By contrast, both catHEC and catDex systems led to only the formation of blue turbid solutions, with the catDex system producing higher turbidity than the catHEC system. Several past studies have established that catHEC polymers can lead to formation of coexisting solid and liquid phases in these systems when the concentration of polymer is increased further.[24,37,39,40,49] Combining the current work with the past work of Miyake and collaborators, we interpret that we observed the relatively narrow region where turbid blue solutions are observed surrounding the solid−liquid phase separation region. As highlighted in the operating diagram measurements presented in Figure 2, the stability window of the blue turbid solution was the widest for model shampoos containing catDex.

We believe that the key difference among the performance of the three cationic polymers in question is related to the overall flexibility of each polymer. Guar has a rigid poly(mannose) backbone with alternating galactose groups. The flexibility of the pendant galactose group is likely constrained by its size and adjacency to the polymer backbone. It is most likely that the cationic group is on the galactose group as shown in Figure 1. While the cellulose backbone is also quite rigid (high persistence length), the cationic groups are most likely at the end of the reactive poly(ethylene oxide) chain pendent to the backbone.[50−52] Mischnick and co-workers demonstrated that commercial grades of HEC contain segments of poly(ethylene oxide) from one to six units in length that extend from the sugar backbone. These pendent poly(ethylene oxide) chains are quite flexible with a persistence length of 0.4 nm,[53] allowing more conformational freedom to the cationic group. The dextran backbone is very flexible, and the cationic groups are either on the backbone itself, or at the end of the occasional short-chain branches (one or two glucose units).[54] From an overall polymer flexibility perspective, the polymers could be ranked from most rigid to least rigid with respect to the cationic groups such as catGuar, catHEC (if the cationic group is bound to the EO chain), and catDex.

Dynamic Light Scattering. The first step toward unmasking the morphology of catDex−surfactant complexes was to measure the average particle size by DLS. First, we characterized the size distribution of surfactant micelles in the absence of catDex at conditions that follow dilution of shampoo at a molar ratio of CapB to SLES 1EO of 0.18. The results are shown in Figure 5. Across the range of dilutions, both intensity and number average particle size distributions showed a single peak below 10 nm-in-diameter. The intensity average particle diameter was 3−4 nm which is consistent with the previously reported size of mixed SLES/CapB spherical micelles.[35]

Next, we repeated the measurement with the catDex polymer added to the system at a mole ratio of polymer to total surfactant of 2×10^{-5} to mimic common use levels in rinse-off personal care products. Again, the samples were prepared to simulate concentrations encountered during dilution of the shampoo. As such, the ratio of polymer to surfactant remained fixed throughout the dilution. The intensity autocorrelation functions provided in Figure S5 of the ESI show that addition of the catDex polymer led to nearly 2 orders of magnitude increase in decay time. The corresponding particle size distributions shown in Figure 5 reveal that particles between 50 and 500 nm-in-diameter are present. The intensity average diameter of the particles ranged between 100 and 200 nm at total surfactant concentrations between 60 and 150 mM. This is much larger than the size of surfactant micelles measured in the absence of the catDex polymer and larger than the diameter expected for a single polymer molecule in solution. Therefore, we proposed that the

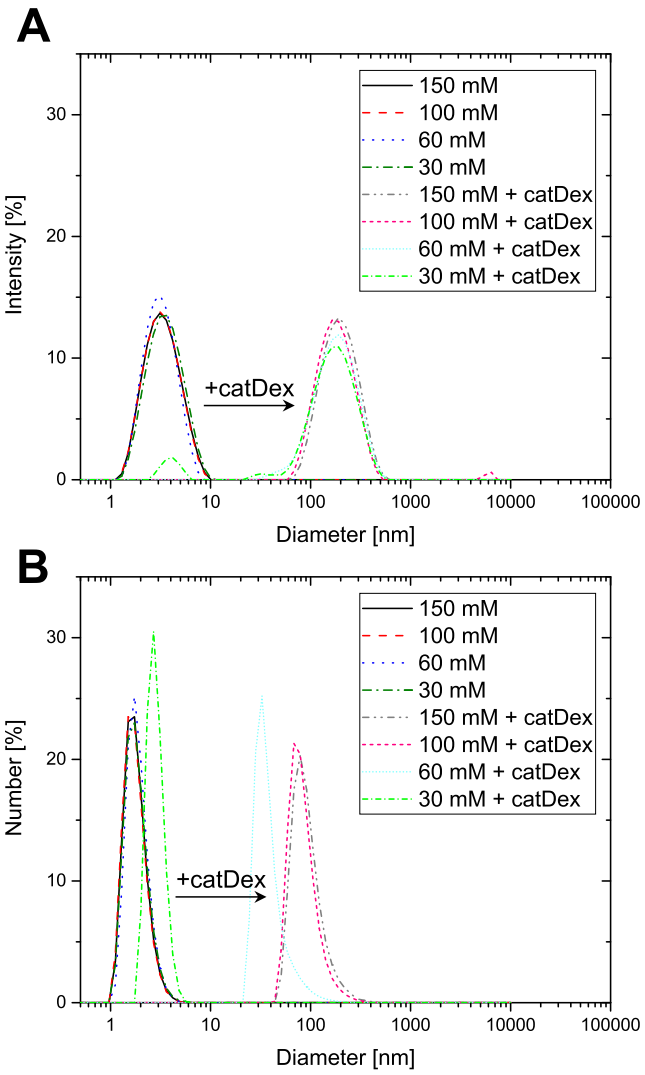

Figure 5. Particle size distributions measured for mixtures SLES 1EO, CapB, and TEA-DDBS in the presence and absence of the catDex polymer by DLS: (A) Intensity average particle size distribution. (B) Number average particle size distribution. The mole ratio of CapB to total surfactant was 0.176, and the mole ratio of TEA-DDBS to total surfactant was 0.008. The mole ratio of the polymer to total surfactant was held constant at 2×10^{-5} for samples with the polymer, corresponding to an approximate charge ratio of 0.013. The legend indicates the total surfactant concentration for each sample.

https://doi.org/10.1021/acs.langmuir.4c02860
Langmuir 2024, 40, 24360−24372

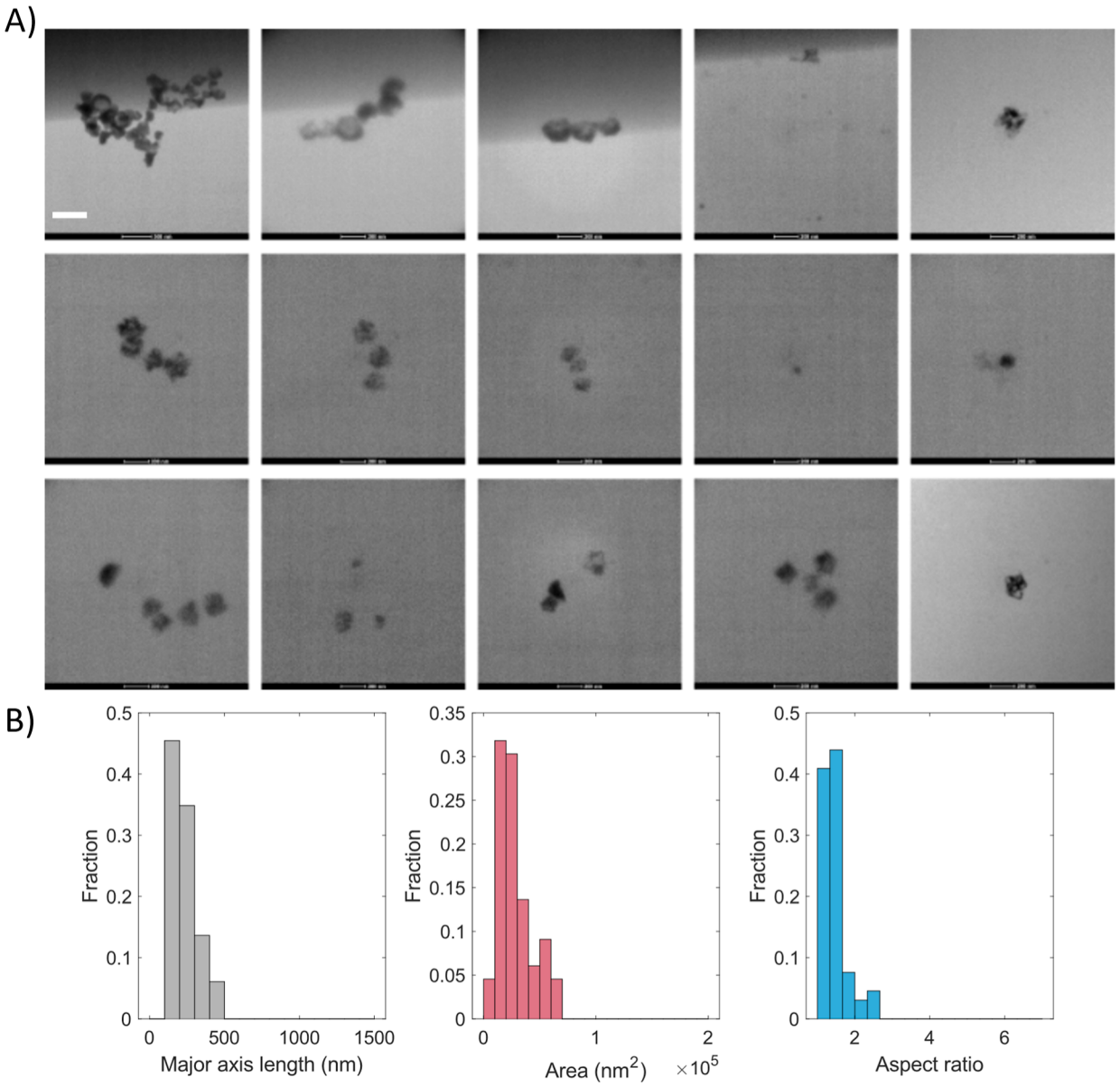

Figure 6. (A) Liquid-phase TEM images of catDex/SLES/CapB nanocomplexes. (B) Statistical results of the shape parameters of the particles formed including the histograms of the major axis, particle areas, and aspect ratio. The scale bar represents 200 nm.

nanometric complexes are polymer−surfactant complexes composed of multiple polymer chains.

The particle size distributions measured for samples with the catDex polymer begin to shift toward smaller particle sizes as dilution occurs. This is more clearly seen in the number average particle size distributions shown in Figure 5B than the intensity average distributions shown in Figure 5A because the number average distributions weight small and large particles equally. The shift toward smaller particle sizes becomes more pronounced at 60 mM total surfactant. At 30 mM total surfactant, two major peaks are observed in the intensity average particle size distribution. The smaller peak is near that of the surfactant in the absence of the catDex polymer. Thus, we interpret these results to indicate that the nanocomplexes disassemble at low dilutions.

Liquid-Phase TEM. While the DLS analysis provides insights into the sizes of the catDex−surfactant complexes and probes the assembled structure in the native liquid environment noninvasively,[55,56] it does not provide detailed real-space imaging, morphology, and spatial heterogeneity information at nanometer length scales. Hence, to further understand the structures of the catDex−SLES/CapB complexes, we utilized liquid-phase TEM methods to quantitatively characterize the real-space imaging of the complexes on the nanometric length scale. As shown in Figure 6A, particulate morphology was observed by liquid-phase TEM throughout the field of view, which can be attributed to the catDex−SLES/CapB complexes. The particles appeared individually or in small clusters, and the individual particles were nonspherical and had an uneven contrast within the particle. This uneven contrast suggests that there was either structural or compositional heterogeneity within the complexes. Further image analysis determined that the catDex−SLES/CapB complexes have an average major axis length of 228 nm, an average particle area of 2.74×10^4 nm,[2] and an average particle aspect ratio of 1.45 as shown in Figure 6B (also refer to Figure S6 for the image

https://doi.org/10.1021/acs.langmuir.4c02860
Langmuir 2024, 40, 24360−24372

segmentation details). Since the liquid-phase TEM analysis is performed in the wet state, it mitigates particle deformation upon drying for soft materials and thus enables a more confident comparison of the particle sizing results with those obtained by other scattering-based techniques such as DLS. In this case, an average major axis length of 228 nm and an aspect ratio of 1.45 measured from the images are in good agreement with the 100−200 nm intensity average diameter determined by the DLS study.

Deposition of Polymer−Surfactant Complexes via QCM-D. The combined results from the DLS and liquid-phase TEM measurements lead us to conclude that the blue turbid solutions observed in catDex−SLES/CapB systems are the result of light scattering from anisotropically shaped complexes with average major axis lengths of ∼200 nm. As mentioned above, polymers are often included in rinse-off personal care formulations to drive deposition and/or deliver hydrophobic materials onto a substrate.[5−9] The target substrates are complex biological systems, such as hair for the case of shampoos. Prior to studying deposition onto hair, we first sought to understand deposition of the catDex−SLES/CapB nanocomplexes onto a simpler model substrate using a QCM-D.

QCM-D is an in situ real-time method with nanoscale accuracy to analyze surface adsorption or deposition of materials onto model surfaces.[57−65] To select the appropriate model surface, we first considered the surface charge of human hair. Slightly damaged hair has a ζ-potential of ∼ −20−40 mV.[66,67] Thus, to model damaged hair, a hydrophilic silica-coated surface was chosen for the QCM-D electrodes (QSense QSX 303 Silicon dioxide sensor). Previously, the ζ-potential of colloidal particles with the same surface nature was measured to be ∼ −42 mV.[57]

To begin the measurements, baseline conditions were established for more than 30 min with Milli-Q water, prior to injection of a dilute model shampoo. Figure 7A shows the adsorption kinetics for catDex−SLES/CapB complexes for a 5-fold dilution of the model shampoo. The figure shows the change in frequency (Δf) of the different overtones of the quartz sensors as a function of time. The viscoelastic nature of the absorbed material can be characterized by two features of the QCM-D results. As shown in Figure 7A, there is a lack of overlapping frequency shifts at different overtones. Note that for a purely elastic film, the results of $\Delta f/\nu$ for all overtones collapse onto a single master curve. Second, for a purely elastic material, the dissipation factor is zero, whereas in Figure 7B, a relatively high value of the dissipation factor (D = 15 ppm) indicates a viscoelastic material.

The dilution-mediated deposition of concentrated catDex−SLES/CapB mixtures is shown in Figure 8. The results showed a decrease in thickness with dilution as shown in Figures 8A, D, and F with Δf_3 and thickness. The results indicate concentration-dependent deposition, whereby deposition decreases as the shampoo is diluted. This behavior contrasts the deposition behavior observed previously for model shampoos formulated with other polysaccharides like catHEC[64] or chitosan,[11,62] where the bulk of deposition takes place in a phase-separated regime during dilution. To provide further insights into the properties of the adsorbed catDex−SLES/CapB nanocomplexes, the viscoelastic properties of the absorbed material were calculated using the Voigt model used previously by Voinova et al.[43,68] Results from measurements at several overtones were fitted to this model

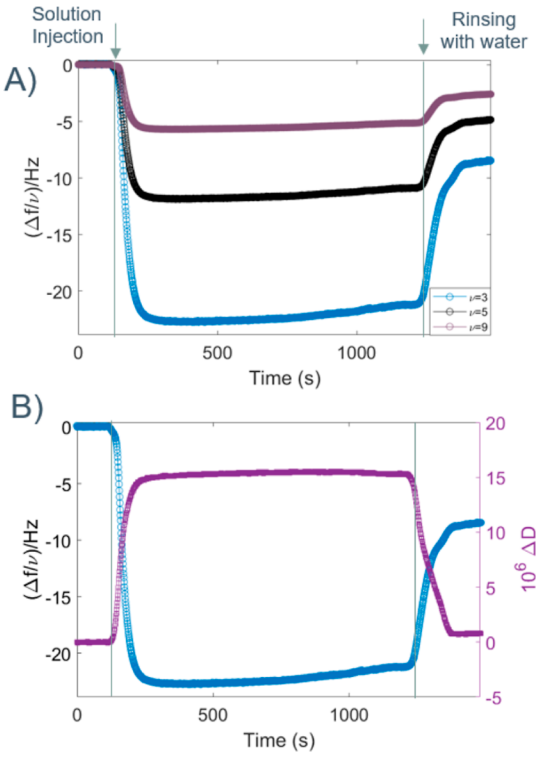

Figure 7. (A) Adsorption kinetics and washout processes for the adsorption of a catDex−SLES/CapB nanocomplex as depicted as the time dependence of the shift of the central frequency of the different overtones of the quart sensors. For clarity, only the curves for ν = 3, 7, and 9 are shown. (B) Time dependence of the $\Delta f/\nu$ and the ΔD for the third overtone. The model shampoo which contained 9 wt % SLES 3EO or 3EO, 2 wt % CapB, and 1.0 wt % polymer was diluted 5-fold with DI water for this measurement.

using the program D-find from QSense (Biolin Scientific). Interestingly, the absorbed complexes from concentrated shampoo demonstrated low elastic modulus values around 3 ± 2 kPa indicating hydrated viscoelastic polyelectrolyte−surfactant complexes of catDex−SLES/CapB. Consequently, these complexes could be an appropriate choice for use in hair care applications to provide softening and conditioning. Further dilution, for example, 20-fold, led to an increase in the elastic modulus, 103 ± 4 kPa, indicating a more compact arrangement on the surface. This hypothesis can be further confirmed by the thickness values shown in Figure 8F, where the thickness value decreases from ∼400 to 7 nm when undiluted shampoo is diluted 20-fold with a concurrent increase in elastic modulus from 3 to 100 kPa.

Polymer-Aided Silicone Deposition via XPS. The QCM-D measurements established that catDex−SLES/CapB nanocomplexes are surface active and capable of depositing onto substrates chosen to mimic some of the surface properties of hair. For commercial rinse-off personal care products, cationic polymers are included to deliver beneficial agents such as silicone emulsions onto hair throughout application and dilution of the product during washing. Based on the QCM-D results, we hypothesized that the anisotropic catDex−SLES/CapB nanocomplexes could drive significantly higher levels of silicone deposition onto hair than commonly used catGuar and catHEC polymers. Thus, we ended this study by formulating model shampoos with the three cationic deposition aid polymers (i.e., catDex, catGuar, or catHEC) according to the

https://doi.org/10.1021/acs.langmuir.4c02860
Langmuir 2024, 40, 24360−24372

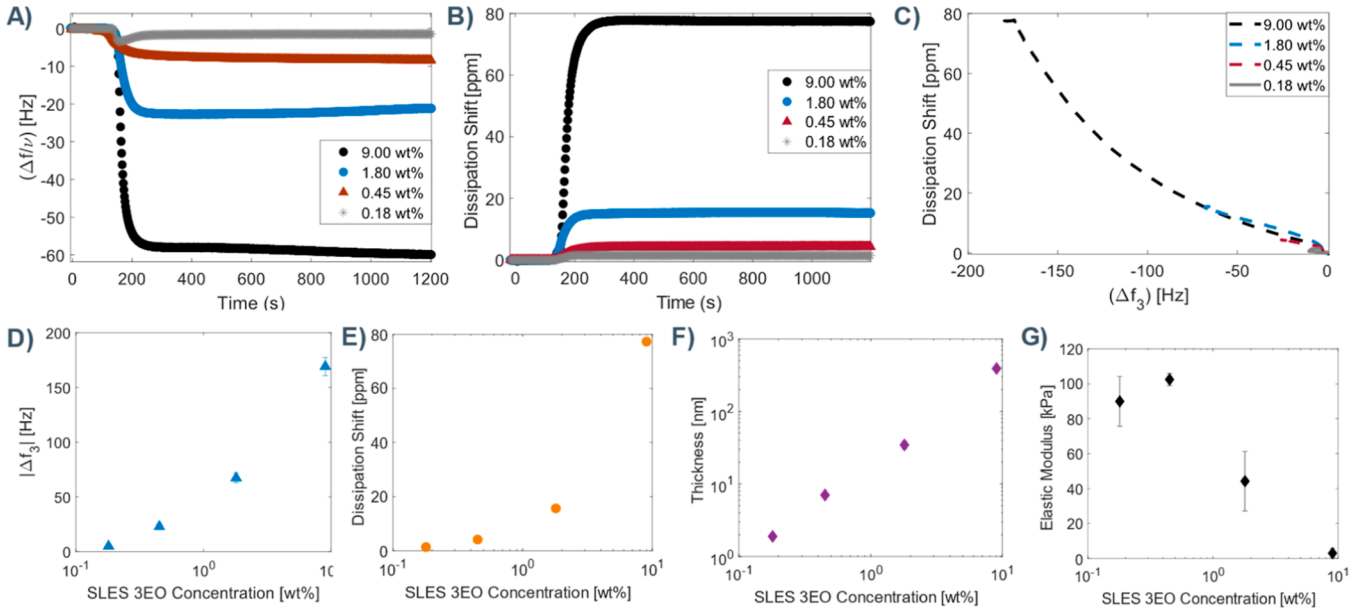

Figure 8. (A,B) Adsorption and dissipation of catDex−SLES 3EO/CapB as depicted by the time dependence shift of the central frequency and dissipation shift of $\nu = 3$ overtone at different dilution. 9.0 wt % refers to concentration of SLES 3EO in a model shampoo, and 1.80, 0.45, and 0.18 wt % refer to 5×, 20×, and 50× diluted shampoo. (C) Δf_3 vs dissipation shift for the third overtone. (D−F) Equilibrium values obtained over three measurements for catDex−SLES/CapB deposition for Δf_3, dissipation shift, and thickness at different dilution. (G) Elastic modulus obtained for a catDex−SLES 3EO/CapB adsorbed layer film on a silica substrate. The error bar represents standard deviation between three repeat experiments.

recipe outlined in Table 2 and characterizing the deposition of the silicone from the shampoos onto hair during washing. After the sheets were washed, XPS was used to quantify silicone deposition onto the tresses.

Figure 9 shows the mole percentage (mol %) of silicon (Si) detected on the surface of virgin brown hair washed with the

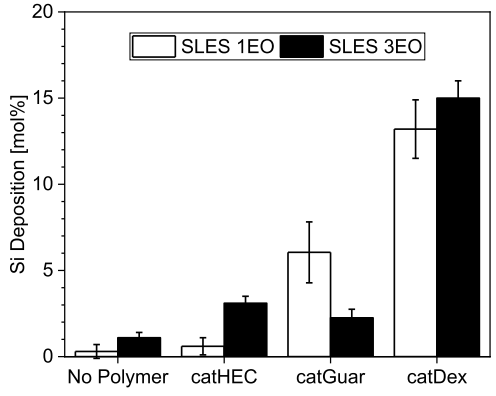

Figure 9. Si deposition measured on the surface of virgin brown hair washed with model shampoo formulations containing catGuar, catHEC, or catDex. The undiluted model shampoos contained 9 wt % SLES 1EO or 3EO, 2 wt % CapB, 0.3 wt % polymer, and 1 wt % silicone from DOWSIL 1785 POE Emulsion.

shampoos. The shampoos formulated with catGuar led to 6.1 ± 1.8 and 2.3 ± 0.5 mol % Si deposition for those containing SLES 1EO and SLES 3EO, respectively. By contrast, catHEC-containing shampoos led to 0.6 ± 0.5 mol % Si deposition onto hair for the case of SLES 1EO and 3.1 ± 0.4 mol % for the case of SLES 3EO. Consistent with our hypothesis, shampoos formulated with the catDex polymer deposited significantly more silicone onto the surface of hair than both catHEC and catGuar. The levels of deposition were 13.2 ± 1.7 and 15.0 ± 1.0 mol % Si from SLES 1EO and SLES 3EO shampoo, respectively. This data directly supports that catDex polymers are a promising technology for replacement of less environmentally friendly catGuar and catHEC polymers. The mechanism by which catDex polymers drive silicone deposition and retention on hair during washing is reported in a separate study.

CONCLUSIONS

The research presented above expanded upon past studies to provide fundamental insights into the size and morphology of complexes formed between catDex polymers and surfactants commonly used in rinse-off personal care applications.[27−32,44] Through a combination of DLS and liquid-phase TEM, it was shown that catDex complexes with SLES/CapB mixtures to form anisotropically shaped particles with an average major length of 228 nm and an aspect ratio of 1.45. Light scattering from these particles leads to a blue, turbid appearance of aqueous solutions throughout compositional spaces relevant to shampoos and body washes. Compared to catHEC and catGuar systems, the blue turbid solutions caused by these nanometric polymer−surfactant complexes can be formed over a much wider range of polymer and surfactant compositions. For catHEC−surfactant systems, the blue turbid solution has been reported previously to form over a narrow compositional space surrounding a solid−liquid miscibility gap.[45] The results presented above are consistent with those of this past study. We believe that the flexibility of the dextran backbone leads to the observed widening of the formulation window over which blue turbid solutions can be obtained.

To understand if the catDex−surfactant complexes could be used to drive deposition in rinse-off personal care applications, we characterized the deposition of the complexes onto a hydrophilic surface with similar zeta potential to damaged hair using QCM-D. We found the complexes to deposit in high amounts throughout a dilution process representative of

https://doi.org/10.1021/acs.langmuir.4c02860
Langmuir 2024, 40, 24360−24372

washing the skin or hair. Based on this observation and the wide range over which the blue turbid solutions can be formed, we propose that this new nanostructure can be leveraged to drive high levels of benefit agent deposition in personal care applications and demonstrate the potential in a model shampoo system. Namely, shampoos formulated with catDex polymers were observed to lead to at least a 2-fold increase in silicone deposited onto hair during washing compared to those formulated with catGuar or catHEC polymers. Exploration of the mechanism of polymer-aided silicone deposition will be the subject of a follow-up study. Overall, the fundamentals described here can be extended to design products beyond personal care, such as electronic materials, pharmaceuticals, biotechnology, and food and nutrition.

■ ASSOCIATED CONTENT

Supporting Information

The Supporting Information is available free of charge at https://pubs.acs.org/doi/10.1021/acs.langmuir.4c02860.

Original images for Figure 2 and Figure 4 of the main text; charge neutralization line sample calculation; dilution of model shampoos formulated with catDex polymers of different MW, different preparation modes to formulate catDex−SLES/CapB model shampoos; autocorrelation functions for DLS; summary of relevant past work using QCM-D to characterize deposition of polymer−surfactant complexes; and liquid-phase transmission electron microscopy image analysis (PDF)

■ AUTHOR INFORMATION

Corresponding Authors

Hammad A. Faizi − *Dow Home & Personal Care, The Dow Chemical Company, Midland, Michigan 48611, United States;* orcid.org/0000-0002-5122-1909; Email: hfaizi@dow.com

Daniel S. Miller − *Core Research & Development, The Dow Chemical Company, Collegeville, Pennsylvania 19426, United States;* orcid.org/0000-0003-3691-2733; Email: dsmiller@dow.com

Authors

Lyndsay Leal − *Dow Home & Personal Care, The Dow Chemical Company, Collegeville, Pennsylvania 19426, United States*

Junsi Gu − *Core Research & Development, The Dow Chemical Company, Collegeville, Pennsylvania 19426, United States*

Michaeleen L. Pacholski − *Core Research & Development, The Dow Chemical Company, Collegeville, Pennsylvania 19426, United States*

Emmett M. Partain III − *Dow Home & Personal Care, The Dow Chemical Company, Collegeville, Pennsylvania 19426, United States*

Caroline Nimako-Boateng − *Core Research & Development, The Dow Chemical Company, Collegeville, Pennsylvania 19426, United States*

Janet R. McMillan − *Core Research & Development, The Dow Chemical Company, Midland, Michigan 48674, United States*

Chang Qian − *Department of Materials Science and Engineering, University of Illinois, Urbana, Illinois 61801, United States*

Zuochen Wang − *Department of Materials Science and Engineering, University of Illinois, Urbana, Illinois 61801, United States;* orcid.org/0000-0002-1150-5931

Qian Chen − *Department of Materials Science and Engineering, University of Illinois, Urbana, Illinois 61801, United States;* orcid.org/0000-0002-1968-441X

Complete contact information is available at: https://pubs.acs.org/10.1021/acs.langmuir.4c02860

Author Contributions

#H.A.F. and D.S.M. authors contributed equally. The manuscript was written through contributions of all authors. All authors have given approval to the final version of the manuscript.

Notes

The authors declare no competing financial interest.

Trademark of The Dow Chemical Company ("Dow") or an affiliated company of Dow.

■ ACKNOWLEDGMENTS

The authors would like to acknowledge John Riley, Thomas Fitzgibbons, Jennifer Todd, Nikhil Fernandes, Maude Desroches, Daniel Almeida, Ashoke Sengupta, Anirudha Banerjee, Beth Johnson, and YuanQiao Rao for useful discussions. The authors would like to acknowledge Yihan Liu for providing critical feedback on the manuscript.

■ REFERENCES

(1) Picken, C. A. R.; Buensoz, O.; Price, P. D.; Fidge, C.; Points, L.; Shaver, M. P. Sustainable formulation polymers for home, beauty and personal care: challenges and opportunities. *Chem. Sci.* **2023**, *14*, 12926−12940.

(2) Luengo, G. S.; Leonforte, F.; Greaves, A.; Rubio, R. G.; Guzman, E. Physico-chemical challenges on the self-assembly of natural and bio-based ingredients on hair surfaces: towards sustainable haircare formulations. *Green Chem.* **2023**, *25*, 7863−7882.

(3) Aguado, R. J.; Mazega, A.; Tarrés, Q.; Delgado-Aguilar, M. The role of electrostatic interactions of anionic and cationic cellulose derivatives for industrial applications: A critical review. *Ind. Crops Prod.* **2023**, *201*, 116898.

(4) Pal, S.; Mal, D.; Singh, R. P. Synthesis and characterization of cationic guar gum: A high performance flocculating agent. *J. Appl. Polym. Sci.* **2007**, *105*, 3240−3245.

(5) Lochhead, R. Y.; Huisinga, L. R.; Waller, T. Deposition from conditioning shampoo: Optimizing coacervate formation. *Cosmet. Toiletries* **2006**, *121*, 75−82.

(6) Miyake, M. Recent progress of the characterization of oppositely charged polymer/surfactant complex in dilution deposition system. *Adv. Colloid Interface Sci.* **2017**, *239*, 146−157.

(7) Svensson, A. V.; Huang, L.; Johnson, E. S.; Nylander, T.; Piculell, L. Surface Deposition and Phase Behavior of Oppositely Charged Polyion/Surfactant Ion Complexes. 1. Cationic Guar versus Cationic Hydroxyethylcellulose in Mixtures with Anionic Surfactants. *ACS Appl. Mater. Interfaces* **2009**, *1*, 2431−2442.

(8) Clauzel, M.; Johnson, E. S.; Nylander, T.; Panandiker, R. K.; Sivik, M. R.; Piculell, L. Surface Deposition and Phase Behavior of Oppositely Charged Polyion−Surfactant Ion Complexes. Delivery of Silicone Oil Emulsions to Hydrophobic and Hydrophilic Surfaces. *ACS Appl. Mater. Interfaces* **2011**, *3*, 2451−2462.

(9) Svensson, A. V.; Johnson, E. S.; Nylander, T.; Piculell, L. Surface Deposition and Phase Behavior of Oppositely Charged Polyion−Surfactant Ion Complexes. 2. A Means to Deliver Silicone Oil to Hydrophilic Surfaces. *ACS Appl. Mater. Interfaces* **2010**, *2*, 143−156.

(10) Llamas, S.; Guzmán, E.; Ortega, F.; Baghdadli, N.; Cazeneuve, C.; Rubio, R. G.; Luengo, G. S. Adsorption of polyelectrolytes and

polyelectrolytes-surfactant mixtures at surfaces: a physico-chemical approach to a cosmetic challenge. *Adv. Colloid Interface Sci.* **2015**, *222*, 461−487.
(11) Fernández-Peña, L.; Guzmán, E. Physicochemical Aspects of the Performance of Hair-Conditioning Formulations. *Cosmetics* **2020**, *7*, 26.
(12) Luengo, G. S.; Fameau, A.-L.; Léonforte, F.; Greaves, A. J. Surface science of cosmetic substrates, cleansing actives and formulations. *Adv. Colloid Interface Sci.* **2021**, *290*, 102383.
(13) Wolff, I. A.; Mehltretter, C. L.; Mellies, R. L.; Watson, P. R.; Hofreiter, B. T.; Patrick, P. L.; Rist, C. E. Production of Clinical-Type Dextran - Partial Hydrolytic Depolymerization and Fractionation of the Dextran from *Leuconostoc mesenteroides* Strain NRRL B-512. *Ind. Eng. Chem.* **1954**, *46*, 370−377.
(14) Burton, B. A.; Brant, D. A. Comparative flexibility, extension, and conformation of some simple polysaccharide chains. *Biopolymers* **1983**, *22*, 1769−1792.
(15) Morris, G. A.; Patel, T. R.; Picout, D. R.; Ross-Murphy, S. B.; Ortega, A.; Garcia de la Torre, J.; Harding, S. E. Global hydrodynamic analysis of the molecular flexibility of galactomannans. *Carbohydr. Polym.* **2008**, *72*, 356−360.
(16) Ferreira, G. A.; Piculell, L.; Loh, W. Addition of *n*-Alcohols Induces a Variety of Liquid-Crystalline Structures in Surfactant-Rich Cores of Dispersed Block Copolymer/Surfactant Nanoparticles. *ACS Omega* **2016**, *1*, 1104−1113.
(17) Ferreira, G. A.; Loh, W. Liquid crystalline nanoparticles formed by oppositely charged surfactant-polyelectrolyte complexes. *Curr. Opin. Colloid Interface Sci.* **2017**, *32*, 11−22.
(18) Chiappisi, L.; Hoffmann, I.; Gradzielski, M. Complexes of oppositely charged polyelectrolytes and surfactants − recent developments in the field of biologically derived polyelectrolytes. *Soft Matter* **2013**, *9*, 3896−3909.
(19) Gradzielski, M.; Hoffmann, I. Polyelectrolyte-surfactant complexes (PESCs) composed of oppositely charged components. *Curr. Opin. Colloid Interface Sci.* **2018**, *35*, 124−141.
(20) Berret, J.-F. Controlling electrostatic co-assembly using ion-containing copolymers: From surfactants to nanoparticles. *Adv. Colloid Interface Sci.* **2011**, *167*, 38−48.
(21) Gradzielski, M. Polyelectrolyte−Surfactant Complexes As a Formulation Tool for Drug Delivery. *Langmuir* **2022**, *38*, 13330−13343.
(22) Kayitmazer, A. B.; Seyrek, E.; Dubin, P. L.; Staggemeier, B. A. Influence of Chain Stiffness on the Interaction of Polyelectrolytes with Oppositely Charged Micelles and Proteins. *J. Phys. Chem. B* **2003**, *107*, 8158−8165.
(23) Goddard, E. D. Polymer—surfactant interaction part II. Polymer and surfactant of opposite charge. *Colloids Surf.* **1986**, *19*, 301−329.
(24) Li, D.; Kelkar, M. S.; Wagner, N. J. Phase Behavior and Molecular Thermodynamics of Coacervation in Oppositely Charged Polyelectrolyte/Surfactant Systems: A Cationic Polymer JR 400 and Anionic Surfactant SDS Mixture. *Langmuir* **2012**, *28*, 10348−10362.
(25) Ghimici, L.; Nichifor, M. Dextran derivatives application as flocculants. *Carbohydr. Polym.* **2018**, *190*, 162−174.
(26) Ghimici, L.; Nichifor, M. Flocculation characteristics of a biodegradable polymer based on dextran. *Sep. Purif. Technol.* **2018**, *194*, 48−55.
(27) Bai, G.; Catita, J. A. M.; Nichifor, M.; Bastos, M. Microcalorimetric Evidence of Hydrophobic Interactions between Hydrophobically Modified Cationic Polysaccharides and Surfactants of the Same Charge. *J. Phys. Chem. B* **2007**, *111*, 11453−11462.
(28) Bai, G.; Nichifor, M.; Lopes, A.; Bastos, M. Thermodynamic Characterization of the Interaction Behavior of a Hydrophobically Modified Polyelectrolyte and Oppositely Charged Surfactants in Aqueous Solution: Effect of Surfactant Alkyl Chain Length. *J. Phys. Chem. B* **2005**, *109*, 518−525.
(29) Bai, G.; Nichifor, M.; Lopes, A.; Bastos, M. Thermodynamics of Self-Assembling of Hydrophobically Modified Cationic Polysaccharides and Their Mixtures with Oppositely Charged Surfactants in Aqueous Solution. *J. Phys. Chem. B* **2005**, *109*, 21681−21689.
(30) Bai, G.; Santos, L. M. N. B. F.; Nichifor, M.; Lopes, A.; Bastos, M. Thermodynamics of the Interaction between a Hydrophobically Modified Polyelectrolyte and Sodium Dodecyl Sulfate in Aqueous Solution. *J. Phys. Chem. B* **2004**, *108*, 405−413.
(31) Nichifor, M.; Bastos, M.; Lopes, S.; Lopes, A. Characterization of Aggregates formed by Hydrophobically Modified Cationic Dextran and Sodium Alkyl Sulfates in Salt-Free Aqueous Solutions. *J. Phys. Chem. B* **2008**, *112*, 15554−15561.
(32) Nichifor, M.; Lopes, S.; Bastos, M.; Lopes, A. Self-Aggregation of Amphiphilic Cationic Polyelectrolytes Based on Polysaccharides. *J. Phys. Chem. B* **2004**, *108*, 16463−16472.
(33) Goddard, E. D. *Principles of Polymer Science and Technology in Cosmetics and Personal Care*; CRC Press, 1999.
(34) Cornwell, P. A. A review of shampoo surfactant technology: consumer benefits, raw materials and recent developments. *Int. J. Cosmet. Sci.* **2018**, *40*, 16−30.
(35) Christov, N. C.; Denkov, N. D.; Kralchevsky, P. A.; Ananthapadmanabhan, K. P.; Lips, A. Synergistic Sphere-to-Rod Micelle Transition in Mixed Solutions of Sodium Dodecyl Sulfate and Cocoamidopropyl Betaine. *Langmuir* **2004**, *20*, 565−571.
(36) Abdel-Rahem, R.; Reger, M.; Hloucha, M.; Hoffmann, H. Rheology of Aqueous Solutions Containing SLES, CAPB, and Microemulsion: Influence of Cosurfactant and Salt. *J. Dispersion Sci. Technol.* **2014**, *35*, 64−75.
(37) Yamaguchi, Y.; Inaba, Y.; Uchiyama, H.; Kunieda, H. Anomalous phase behavior of water-soluble polyelectrolyte and oppositely charged surfactants. *Colloid Polym. Sci.* **1999**, *277*, 1117−1124.
(38) Ghasemi, M.; Jamadagni, S. N.; Johnson, E. S.; Larson, R. G. A Molecular Thermodynamic Model of Coacervation in Solutions of Polycations and Oppositely Charged Micelles. *Langmuir* **2023**, *39*, 10335−10351.
(39) Goddard, E. D.; Hannan, R. B. Polymer/surfactant interactions. *J. Am. Oil Chem. Soc.* **1977**, *54*, 561−566.
(40) Goddard, E. D.; Hannan, R. B. Cationic polymer/anionic surfactant interactions. *J. Colloid Interface Sci.* **1976**, *55*, 73−79.
(41) Kalantar, T. H.; et al. High throughput workflow for coacervate formation and characterization in shampoo systems. *J. Cosmet. Sci.* **2017**, *4*, 375−384.
(42) Faizi, H. A.; Frey, S. L.; Steinkühler, J.; Dimova, R.; Vlahovska, P. M. Bending rigidity of charged lipid bilayer membranes. *Soft Matter* **2019**, *15*, 6006−6013.
(43) Voinova, M. V.; Rodahl, M.; Jonson, M.; Kasemo, B. Viscoelastic Acoustic Response of Layered Polymer Films at Fluid-Solid Interfaces: Continuum Mechanics Approach. *Phys. Scr.* **1999**, *59*, 391−396.
(44) Miyake, M.; Kakizawa, Y. Morphological study of cationic polymer−anionic surfactant complex precipitated in solution during the dilution process. *Int. J. Cosmet. Sci.* **2010**, *32*, 473.
(45) Kakizawa, Y.; Miyake, M. Creation of New Functions by Combination of Surfactant and Polymer - Complex Coacervation with Oppositely Charged Polymer and Surfactant for Shampoo and Body Wash -. *J. Oleo Sci.* **2019**, *68*, 525−539.
(46) Mezei, A.; Mészáros, R.; Varga, I.; Gilányi, T. Effect of Mixing on the Formation of Complexes of Hyperbranched Cationic Polyelectrolytes and Anionic Surfactants. *Langmuir* **2007**, *23*, 4237−4247.
(47) Guzmán, E.; Fernández-Peña, L.; Ortega, F.; Rubio, R. G. Equilibrium and kinetically trapped aggregates in polyelectrolyte−oppositely charged surfactant mixtures. *Curr. Opin. Colloid Interface Sci.* **2020**, *48*, 91−108.
(48) Desmond Goddard, E.; Gruber, J. V. *Principles of Polymer Science and Technology in Cosmetics and Personal Care*; CRC Press: London, 2005..
(49) Regismond, S. T. A.; Winnik, F. M.; Goddard, E. D. Surface viscoelasticity in mixed polycation anionic surfactant systems studied

https://doi.org/10.1021/acs.langmuir.4c02860
Langmuir 2024, 40, 24360−24372

by a simple test. *Colloids Surf. A: Physicochem. Eng. Asp.* **1996**, *119*, 221−228.
(50) Adden, R.; Müller, R.; Brinkmalm, G.; Ehrler, R.; Mischnick, P. Comprehensive Analysis of the Substituent Distribution in Hydroxyethyl Celluloses by Quantitative MALDI-ToF-MS. *Macromol. Biosci.* **2006**, *6*, 435−444.
(51) Mischnick, P.; Unterieser, I.; Voiges, K.; Cuers, J.; Rinken, M.; Adden, R. A New Method for the Analysis of the Substitution Pattern of Hydroxyethyl(methyl)-Celluloses Along the Polysaccharide Chain. *Macromol. Chem. Phys.* **2013**, *214*, 1363−1374.
(52) Mischnick, P. Analysis of the Substituent Distribution in Cellulose Ethers − Recent Contributions. In *Cellulose Science and Technology: Chemistry, Analysis, and Applications*; Wiley, 2018; pp 143−173..
(53) Dalhaimer, P.; Blankenship, K. R. All-Atom Molecular Dynamics Simulations of Polyethylene Glycol (PEG) and LIMP-2 Reveal That PEG Penetrates Deep into the Proposed CD36 Cholesterol-Transport Tunnel. *ACS Omega* **2022**, *7*, 15728−15738.
(54) Pasika, W. M.; Cragg, L. H. The Detection and Estimation of Branching in Dextran by Proton Magnetic Resonance Spectroscopy. *Can. J. Chem.* **1963**, *41*, 293−299.
(55) Li, T.; Senesi, A. J.; Lee, B. Small Angle X-ray Scattering for Nanoparticle Research. *Chem. Rev.* **2016**, *116*, 11128−11180.
(56) Kim, J.; Jones, M. R.; Ou, Z.; Chen, Q. In Situ Electron Microscopy Imaging and Quantitative Structural Modulation of Nanoparticle Superlattices. *ACS Nano* **2016**, *10*, 9801−9808.
(57) Guzmán, E.; Ortega, F.; Baghdadli, N.; Cazeneuve, C.; Luengo, G. S.; Rubio, R. G. Adsorption of Conditioning Polymers on Solid Substrates with Different Charge Density. *ACS Appl. Mater. Interfaces* **2011**, *3*, 3181−3188.
(58) Guzmán, E.; Ortega, F.; Baghdadli, N.; Luengo, G. S.; Rubio, R. G. Effect of the molecular structure on the adsorption of conditioning polyelectrolytes on solid substrates. *Colloids Surf., A* **2011**, *375*, 209−218.
(59) Merta, J.; Tammelin, T.; Stenius, P. Adsorption of complexes formed by cationic starch and anionic surfactants on quartz studied by QCM-D. *Colloids Surf., A* **2004**, *250*, 103−114.
(60) Tammelin, T.; Merta, J.; Johansson, L.-S.; Stenius, P. Viscoelastic Properties of Cationic Starch Adsorbed on Quartz Studied by QCM-D. *Langmuir* **2004**, *20*, 10900−10909.
(61) Guzmán, E.; Ritacco, H.; Rubio, J. E. F.; Rubio, R. G.; Ortega, F. Salt-induced changes in the growth of polyelectrolyte layers of poly(diallyl-dimethylammonium chloride) and poly(4-styrene sulfonate of sodium). *Soft Matter* **2009**, *5*, 2130−2142.
(62) Puente-Santamaría, A.; Monge-Corredor, J.; Ortega, F.; Rubio, R. G.; Guzmán, E. Dilution-controlled deposition of mixtures of a synthetic polycation and a natural origin polyelectrolyte with anionic surfactants on negatively charged surfaces. *Colloids Surf., A* **2024**, *685*, 133137.
(63) Naderi, A.; Claesson, P. M. Adsorption Properties of Polyelectrolyte−Surfactant Complexes on Hydrophobic Surfaces Studied by QCM-D. *Langmuir* **2006**, *22*, 7639−7645.
(64) Dhopatkar, N.; Park, J. H.; Chari, K.; Dhinojwala, A. Adsorption and Viscoelastic Analysis of Polyelectrolyte−Surfactant Complexes on Charged Hydrophilic Surfaces. *Langmuir* **2015**, *31*, 1026−1037.
(65) Terada, E.; Samoshina, Y.; Nylander, T.; Lindman, B. Adsorption of Cationic Cellulose Derivative/Anionic Surfactant Complexes onto Solid Surfaces. II. Hydrophobized Silica Surfaces. *Langmuir* **2004**, *20*, 6692−6701.
(66) McMullen, R. L.; Laura, D.; Zhang, G.; Kroon, B. Investigation of the interactions of cationic guar with human hair by electrokinetic analysis. *Int. J. Cosmet. Sci.* **2021**, *43*, 375−390.
(67) Jachowicz, J.; Maxey, S.; Williams, C. Sorption/desorption of ions by dynamic electrokinetic and permeability analysis of fiber plugs. *Langmuir* **1993**, *9*, 3085−3092.
(68) Voinova, M. V.; Jonson, M.; Kasemo, B. Missing mass' effect in biosensor's QCM applications. *Biosens. Bioelectron.* **2002**, *17*, 835−841.

https://doi.org/10.1021/acs.langmuir.4c02860
Langmuir 2024, 40, 24360−24372